Atmos. Chem. Phys. Discuss., 14, 22245–22272, 2014
www.atmos-chem-phys-discuss.net/14/22245/2014/
doi:10.5194/acpd-14-22245-2014

Atmospheric Chemistry and Physics Discussions

First quasi-Lagrangian in-situ measurements of Antarctic Polar springtime ozone: observed ozone loss rates from the Concordiasi long-duration balloon campaign

R. Schofield[1,2], L. M. Avallone[3,4], L. E. Kalnajs[3], A. Hertzog[5], I. Wohltmann[6], and M. Rex[6]

[1]School of Earth Sciences, University of Melbourne, Melbourne, Australia
[2]ARC Centre of Excellence for Climate System Science, University of New South Wales, New South Wales, Australia
[3]Laboratory for Atmospheric and Space Physics, University of Colorado, Boulder, USA
[4]National Science Foundation, Washington, USA
[5]Laboratoire de Météorologie Dynamique, Palaiseau, France
[6]Alfred Wegener Institute, Potsdam, Germany

Received: 14 July 2014 – Accepted: 13 August 2014 – Published: 1 September 2014

Correspondence to: R. Schofield (robyn.schofield@unimelb.edu.au) and
L. M. Avallone (linnea.avallone@colorado.edu)

Published by Copernicus Publications on behalf of the European Geosciences Union.

ACPD
14, 22245–22272, 2014

Abstract

We present ozone measurements made using state-of-the-art ultraviolet photometers onboard three long-duration stratospheric balloons launched as part of the Concordiasi campaign in austral spring 2010. Ozone loss rates calculated by matching air-parcels sampled at different times and places during the polar spring are in agreement with rates previously derived from ozonesonde measurements, for the vortex-average, ranging between 2–7 ppbv (sunlit h)$^{-1}$ or 25–110 ppbv per day. However, the geographical coverage of these long-duration stratospheric balloon platforms provides new insights into the temporal and spatial patterns of ozone loss over Antarctica. Very large ozone loss rates of up to 200 ppbv day^{-1} (16 ppbv (sunlit h)$^{-1}$) are observed for airmasses that are down-wind of the Antarctic Peninsula and/or over the East Antarctic region. The ozone loss rate maximum downstream of the Antarctic Peninsula region is consistent with high PSC occurrence from Calipso and large ClO abundances from MLS satellite observations for 12–22 September 2010.

1 Introduction

26 years after the signing of the Montreal Protocol, widely considered the most successful international environmental policy of our time, there is evidence that stratospheric chlorine – the primary anthropogenic contributor to stratospheric ozone loss – is returning to pre-human-influence levels. In addition, the climate protection due to the reduction of chlorofluorocarbons, halons and methyl bromide mandated by the Montreal Protocol exceeds carbon mitigation strategies to date. Despite these successes, important questions have remained unanswered because of the technological challenges of directly measuring stratospheric ozone losses in-situ.

Stratospheric ozone, and its dramatic annual losses in the Antarctic spring, have been shown to have a strong influence over the entire southern hemispheric climate (Thompson et al., 2011). The effects include the suppression in the expected warming

ACPD
14, 22245–22272, 2014

of the Antarctic region (Thompson and Solomon, 2002) due to increasing greenhouse gas levels and a strengthening of the polar jet. Due to the significant chlorine reductions brought about by the Montreal Protocol, polar springtime stratospheric ozone losses are expected to return to pre-1980 levels by 2050 (Bekki et al., 2011), and consequently, the role of stratospheric ozone in modulating the Southern Hemisphere climate will change during this time period. Conversely, the formation of polar stratospheric clouds (PSCs), crucial in converting chlorine from reservoir species into active radicals, has been linked to tropospheric cloud systems. Kohma and Sato (2013) demonstrate that, in 2010, 33 % of PSCs between 15 and 20 km were associated with the radiative cooling resulting from blocking anticyclones and clouds in the troposphere. Thus the changing climate, which affects the presence of tropospheric cloud systems, also modulates stratospheric ozone loss.

While the overall chemical scheme for the polar ozone loss process is now well understood, reconciliation of some of the details of the kinetics is vital, as these define the extent of ozone loss and the evolution of the ozone hole in a future atmosphere with higher greenhouse gas levels and colder stratospheric temperatures. Polar stratospheric ozone loss occurs predominantly as a result of the ClO dimer catalytic cycle that operates in the low UV conditions of the lower stratosphere (Molina and Molina, 1987; Solomon, 1999), where other radicals such as atomic oxygen are not present:

$$\mathrm{ClO + ClO + M \leftrightharpoons ClOOCl + M} \quad \text{(R1)}$$

$$\mathrm{ClOOCl + h\nu \longrightarrow Cl + ClOO} \quad \text{(R2)}$$

$$\mathrm{ClOO + M \longrightarrow Cl + O_2 + M} \quad \text{(R3)}$$

$$\mathrm{2 \times (Cl + O_3 \longrightarrow ClO + O_2)} \quad \text{(R4)}$$

$$\text{Net:} \quad \mathrm{2\,O_3 \longrightarrow 3\,O_2}$$

Some questions still remain about the kinetics of this cycle because laboratory measurements and results obtained from in situ observations differ, although this gap is closing. For example, the equilibrium constant given by Reaction (R1) when derived from the atmospheric observations has consistently been observed to be smaller than

ACPD
14, 22245–22272, 2014

laboratory estimates (Avallone and Toohey, 2001; Stimpfle et al., 2004; von Hobe et al., 2005; Schofield et al., 2008; Santee et al., 2010). Recently, the photolysis rate of the ClO dimer (Reaction R2) underwent much scrutiny in the laboratory following the publication of a very low rate by Pope et al. (2007). It has since been shown that the Cl_2 correction applied was causing this low laboratory rate, and now laboratory rates converge on higher values (Chen et al., 2009; von Hobe et al., 2009; Papanastasiou et al., 2009; Wilmouth et al., 2009). These higher photolysis rate estimates are consistent with rates either measured directly in the atmosphere or derived from atmospheric observations (Shindell and deZafra, 1996; Avallone and Toohey, 2001; Solomon et al., 2002; Vogel et al., 2003; Stimpfle et al., 2004; von Hobe et al., 2007; Schofield et al., 2008; Kremser et al., 2011). While the JPL 2011 (Sander et al., 2011) recommendation for chemical and photochemical rates is now for the larger Papanastasiou et al. (2009) cross-section, for the first time, the panel recommends a quantum yield of 0.9 (previously 1.0) for the photolysis reaction given by Reaction (R2) and a 10 % channel for direct ClO production, which will be more rapid than thermal decomposition of the dimer via reverse Reaction (R1). With a quantum yield of 0.9 the ozone loss due to the dimer cycle is reduced by 5 % (Plenge et al., 2004). Thus taking into account a non-unity quantum yield will require either higher total inorganic chlorine Cl_y or higher dimer cross-section or smaller k_f associated with dimer formation (Reaction R1) to explain previously observed ozone loss rates.

Ozone loss rates have been successfully derived by following and matching distinct airmasses in time using many ozonesondes during intensive "Match" campaigns in the Arctic and the Antarctic (Rex et al., 1998, 2002). A similar approach of matching airmasses using observations from the POAM II (Bevilacqua et al., 1997) and III (Hoppel et al., 2005) satellites found 85 ± 15 ppbv day^{-1} (1994–1996) and 8 ± 6 ppbv (sunlit h)$^{-1}$ (1998–2003), respectively. For the more recent time period a vortex-average of 45 ± 6 ppbv day^{-1} has been derived from the SCIAMACHY satellite observations (Sonkaew et al., 2013). Hassler et al. (2011) used ozonesonde measurements at the South Pole to derive rates of 90 ± 10 and 70 ± 10 ppbv day^{-1} for 1991–1995 and 1996–2010 peri-

ACPD
14, 22245–22272, 2014

ods, respectively. Observations at one fixed location do not deliver rates representative of the true in-situ loss, but compare very well to vortex-average loss rates. Using the air-mass match technique, vortex-averaged Antarctic ozone losses of 4 ± 1 ppbv (sunlit h)$^{-1}$ were observed from 15 August to 15 September in 2002 by Frieler et al. (2006). Ozone loss rates for the total column have been derived from the ground-based Dobson/Brewer/SAOZ network (Kuttippurath et al., 2010) to be 2.5 ± 0.5 DU day^{-1} (13 August 2005–2 October 2009), in good agreement with SCIAMACHY, 2.0 ± 0.3 DU day^{-1}, for the same time period and OMI, 2.4 ± 0.5 DU day^{-1}, for a shorter time period (18 August 2002–18 September 2008). While these column loss rates are not directly comparable to in situ loss rates they are provided for completeness here, as the column loss rates influence surface UV, hence the biosphere and health implications of ozone loss. Questions remain about the details of ozone loss and, in particular, about loss rates during the earliest stages of ozone depletion, particularly cold Arctic January losses. We show in this paper that both the spatial and temporal variations of the ozone loss rates in the Antarctic need to be considered, moving away from vortex-average loss rates view.

This paper presents for the first time ozone loss rates measured in situ onboard quasi-Lagrangian balloons and is organised as follows. The following section provides details of the measurements. The modelling section details the match analysis and ozone loss rates derived for the balloon flights. These are then compared to previous estimates of ozone loss rates and discussed in the last section.

2 Measurements

For the first time ozone loss has been observed in situ over long periods of time by specially designed ultraviolet photometers (Kalnajs and Avallone, 2010) flown on long duration balloons launched as part of the Concordiasi campaign (Rabier et al., 2013) out of McMurdo Station, Antarctica in austral spring of 2010. These super-pressure balloons travel on constant density (isopycnic) surfaces; the 2010 Concordiasi pay-

ACPD
14, 22245–22272, 2014

loads were launched to a density $\rho = 115\,\mathrm{g\,m^{-3}}$ which corresponds to approximately 65 hPa (17 km). Of the nineteen balloons launched during Concordiasi, six (designated PSC-14 through 19) carried payloads with sensors to measure state parameters (T, p), ozone, and either particle size distribution via optical scattering or temperature profiles via GPS occultation. Ozone instruments were built by two groups – one at the Laboratoire de Météorologie Dynamique in Paris, France, hereafter referred to as LMDOz, and one at the University of Colorado Boulder, hereafter designated UCOz. Four of the six ozone balloons additionally carried laser particle counters from the University of Wyoming. Ward et al. (2014) showed that data from the PSC-15 balloon gondola indicate particles consistent with nitric acid trihydrate (NAT) formation only 2 days after the temperature (T_{NAT}) threshold had been reached.

The six payloads returned data every 15–30 min for periods ranging from 6 to 96 days; in all cases, the end of the data record was the result of communications failure with the payload rather than of instrument failure. By careful control of the balloon descent, three of the six payloads were unexpectedly recovered and the ozone sensors were returned to the laboratory for post-flight testing and calibration. In all cases, the post-flight diagnostics indicated that no degradation had taken place during flight and that the calibrations remained stable. Therefore, the ozone data discussed here are accurate to 20 ppb. The accuracy of the ozone instruments in flight was validated through coordinated ozonesonde launches from several Antarctic research stations. Ozone sondes were launched from each station when a PSC flight passed near the station; 12 comparisons between sonde and long duration ozone data were performed, with 5 concurrent comparisons having a separation of less than 100 km.

Data from three ozone instruments – those called PSC-14, PSC-16 and PSC-17 – are discussed in the analysis below. PSC-15 had a very short lifetime due to a battery failure on the balloon gondola. PSC-18 and PSC-19 were launched on 29 September and 8 October, respectively, after the majority of the ozone loss had taken place. Details of the three flights reported on here are given in Table 1.

ACPD
14, 22245–22272, 2014

2.1 Trajectories and match criteria

The balloon trajectories displayed in Fig. 1 show that it takes approximately 10 days for the balloon to circumnavigate the Antarctic stratosphere. Figure 2 displays the ozone measurements and the corresponding potential temperature surfaces for the three trajectories shown in Fig. 1. The balloons are not perfect tracers of air motion. First, the Concordiasi balloons follow isopycnic surfaces rather than constant potential temperature (isentropic) surfaces. Furthermore, the diurnal heating and cooling of the balloons produces clear diurnal variations in the potential temperatures. Care was therefore taken when matching the air-parcels to calculate the ozone loss. These variations were important because horizontal distances travelled between air-parcels of different potential temperature (even a few K apart) can be very large, due to the large wind shears and velocities occurring in the stratospheric polar vortex – hence strict air-mass match criteria were applied.

Back-trajectories were generated using ATLAS (Wohltmann and Rex, 2008) driven by ERA-Interim meteorology and total radiative heating rates. The trajectories were initiated every 15 min along the balloon flight path and calculated backwards until the balloon launch time. The trajectories were saved at 30 min intervals.

Match pairs were defined following the definitions of Rex et al. (1999): each of the match pairs must satisfy the following difference criteria: < 1 K potential temperature, $< 1\,s^{-1}$ potential vorticity and < 10 days in time. The match radius (shortest distance between trajectory and balloon location) must be < 300 km and the normalised potential vorticity (PV) along the entire trajectory must be $< -36\,s^{-1}$ to ensure that the match occurs within the Antarctic polar vortex. The normalised PV is calculated using the

ACPD
14, 22245–22272, 2014

following function:

$$\mathrm{PV_{Norm}} = -0.265\frac{PV}{\mathrm{PV_{Scale}}} \quad (1)$$

$$\mathrm{PV_{Scale}} = \frac{0.0981}{(b + 2c\theta + 3d\theta^2)\exp^{(\ln P)}} \quad (2)$$

$$\ln P = a + b\theta + c\theta^2 + d\theta^4 \quad (3)$$

where θ is the potential temperature and the parameters $a = 12.48$, $b = -3.212\times10^{-2}$, $c = 3.708\times10^{-5}$, $d = -1.627\times10^{-8}$ have been established from the relationship among pressure, theta and PV from Antarctic ozonesonde matches.

To determine the ozone loss rate, a regression of the change in ozone vs. sunlit hours or days for a number of matches was performed. After application of the match criteria, matches were binned according to the time period over which they sampled; i.e., when a match pair spanned days 264 to 272 it would be binned in the 255–265, 260–270 and 265–275 bins. More than 10 matches were required for a regression slope to be determined. As there was little potential temperature-dependence of the ozone loss rates (and theta varied maximally 20 K over the balloon lifetime), all matches were included, ignoring the potential temperature of the match. So while the potential temperature was important for determining the match, the resultant ozone loss rates were not sensitive to it.

3 Results and discussion

Analysis of the 2010 ozone hole by Klekociuk et al. (2011) shows it to be a one of the smallest in area since the discovery of the ozone hole. However, the total ozone loss in the lowermost stratosphere was seen to be similar to losses that occurred in previous recent years. Therefore the losses observed in 2010 can be seen as representative of perturbed springtime Antarctic ozone losses. There was very little dynamical dis-

ACPD
14, 22245–22272, 2014

turbance of the polar vortex after September; thus the rates observed by Concordiasi were not influenced by a premature break-up. In fact 2010 was one of the longest-lasting ozone holes on record, persisting into December.

Figures 3 and 4 display the ozone loss rates per sunlit hour and per day, respectively, determined by binning according to the latitude of the end match point. The four latitude quadrant bins are shown in the map insets (with their associated colours used in the line plot). Maximum ozone loss rates are observed in the early time periods for matches that end in the 0–90° W quadrant (depicted in red) of Antarctica – the Antarctic Peninsula region for balloon PSC-17 – and the 90–180° W quadrant (depicted in yellow) – Ross Sea and Marie Byrd Land region for balloon PSC-16. The 0–90° E quadrant (blue) showed the largest losses in the later time periods. The ozone losses were very large for the earliest time period of 255–265 day of year (11–21 September). This is consistent with air-masses having PSC contact in the previous quadrants over East Antarctica (0–90° E). PSCs have been shown to have a higher incidence over the central and Antarctic Peninsula regions for altitudes between 15–20 km and are highly correlated with tropospheric systems that have clouds that reach above 7.5 km (Wang et al., 2008).

The balloon trajectories (Figs. 1 and 3) show that the PSC-16 and PSC-17 balloons were largely displaced off the continent while in the 0–90° E and 0–90° W quadrants, respectively. As a result, these airmasses would have experienced larger exposures to sunlight at these northern latitudes. For PSC-16 this translated into higher ozone losses with match latitude (Fig. 5, middle panel) but for PSC-17 the extreme ozone losses can not be attributed to more sunlight exposure (Fig. 5, lower panel). For this balloon, the more negative mean PV values of the matches are associated with the large ozone losses (Fig. 6). The PV displayed in Fig. 6 are normalised thus more negative PV are associated with higher vorticities. Unfortunately, there are not sufficient statistics to determine this relationship for PSC-16. PSC-16 experienced the largest ozone losses when the match end point was in the 90–180° W sector (Ross Sea and Marie Byrd Land) thus, it is likely that the exposure to higher sunlight at northern latitudes drove

ACPD
14, 22245–22272, 2014

these losses and maintained the high ClO that was observed for PSC-16 over the days 260–270.

To understand the low sunlight exposure, yet very high ozone losses, for matches ending between days 255 and 265 seen by the PSC-17 balloon, examining the chlorine activation, as evidenced by the abundance of ClO (Fig. 7), and PSC area (Fig. 8) was necessary. The PSC-17 flight passed over the Antarctic Peninsula then stayed over the continent between days 255 and 265. ClO observations from the microwave limb sounder (MLS) onboard the Aura satellite (Santee et al., 2008) at 68.13 hPa showed zonal symmetry for the day 255–265 time period, which is absent in the later time periods when the vortex was largely displaced toward the 0–90° E sector.

The PSC data from the CALIOP (Cloud–Aerosol LIdar with Orthogonal Polarization) onboard the CALIPSO (Cloud–Aerosol Lidar and Infrared Pathfinder Satellite Observations) satellite (Pitts et al., 2009) is shown in Fig. 8. This shows that PSCs were present downwind of the Antarctic Peninsula region and largely absent from the Ross Sea region, 90–180° E and 90–180° W, respectively. So PSC-17 had maximum exposure to the Antarctic Peninsula PSC region and subsequently high ClO in the air-masses that it sampled. The resulting ozone losses of around 230 ppbv day^{-1} were seen for matches that had end points in the Antarctic Peninsula sector (i.e., airmasses have passed over the Peninsula mountains where large excursions of temperature and resulting PSC formation are known to take place), at latitudes poleward of 75° S and potential vorticities between −58 and −62 s^{-1}. This result is also consistent with the findings of Kohma and Sato (2013) who attribute a 20 % probability of PSC formation due to anticyclonic clouds in the troposphere for September (it is higher for the winter months). The Antarctic Peninsula, but also Marie Byrd Land, are cited as important geographical regions for PSC formation.

Table 2 compares the ozone loss rates calculated here with those found previously in the literature for the Antarctic region. The vortex-average values from Concordiasi are in good agreement with the ozonesonde match campaign held in 2003 and satellite estimates from POAM III and Sciamachy. Comparisons with ozone losses determined

ACPD
14, 22245–22272, 2014

from sondes launched at a single station also show consistency. However, what is hidden in the vortex-average is how fast the ozone loss can be over the geographic region of the Antarctic Peninsula when conditions are favourable. Losses of up to 230 ppbv day^{-1} are exceptional and dictate the speed at which the ozone hole forms in early September.

4 Conclusions

Ozone loss rates were derived from the Concordiasi quasi-Lagrangian long duration balloons flown at 17 km (65 hPa) over Antarctica in September of 2010, which carried instrumentation that measured ozone continuously in-situ for the first time. The loss rates were similar to previously reported Antarctic vortex-average loss rates of 6 ± 6 ppbv (sunlit h)$^{-1}$ or 74 ± 70 ppbv per day. However, exceptionally rapid ozone loss rates of 230 ppbv per day (20 ppbv (sunlit h)$^{-1}$) were observed for airmasses that traversed the Antarctic Peninsula region while remaining at high latitudes and high absolute PV. This geographical maximum in the ozone loss rates is consistent with high PSC occurrence and large ClO abundances present during 12–22 September as observed from Calipso and MLS, respectively, downstream of the Antarctic Peninsula region.

Previous studies of Antarctic ozone loss rates have considered vortex-average losses exclusively. By moving away from this view, these high fidelity Concordiasi ozone observations and derived ozone loss rates downstream of the Antarctic Peninsula can be used to test the ability of chemistry climate models to capture the timing and spatial variations of ozone hole formation. A comparison of these loss rates and chemical transport simulations using laboratory based reaction rates is beyond the scope of this paper, and makes up a future study that explores the chlorine dimer kinetics and their uncertainties.

These high fidelity ozone measurements onboard long duration balloon flights have provided valuable spatial insight into Antarctic polar ozone loss. If the google loon project (www.google.com/loon/) becomes operational providing coverage of the South-

ACPD
14, 22245–22272, 2014

ern Hemisphere and instrumented with ozone sensors such as those used in Concordiasi, the potential for in situ insights into mid to high-latitude ozone chemistry in the lowermost stratosphere will be possible. This is a region where satellite retrievals are challenged and questions concerning the ozone loss rates on cold stratospheric aerosol could potentially be addressed.

Acknowledgements. Concordiasi is an international project, currently supported by the following agencies: Météo-France, CNES, CNRS/INSU, NSF, NCAR, University of Wyoming, Purdue University, University of Colorado, the Alfred Wegener Institute, the Met Office, and ECMWF. Concordiasi also benefits from logistic or financial support of the operational polar agencies Institut Polaire Français Paul Emile Victor (IPEV), Programma Nazionale di Ricerche in Antartide (PNRA), United States Antarctic Program (USAP) and British Antarctic Survey (BAS), and from Baseline Surface Radiation Network (BSRN) measurements at Concordia. Concordiasi is part of The Observing System Research and Predictability Experiment-International Polar Year (THORPEX-IPY) cluster within the International Polar Year effort. The Concordiasi website can be found at www.cnrm.meteo.fr/concordiasi/. The PSC mask data from the Calipso instrument were obtained from the NASA Langley Research Center Atmospheric Science Data Center. The Microwave Limb Sounder ClO data were obtained from Nathaniel Livesey. The authors thank ECMWF for providing ERA-Interim data via special project DERESI. RS received funding support for this work from the European Union (EU) WaVES (MIF1-CT-2006–039646) project, Australian Antarctic Science Grant (FoRCES 4012) and the Australian Research Council's Centre of Excellence (CE110001028) scheme. LMA and LEK acknowledge support from the US National Science Foundation under grant ANT-0839017.

References

Avallone, L. and Toohey, D.: Tests of halogen photochemistry using in situ measurements of ClO and BrO in the lower polar stratosphere, J. Geophys. Res., 106, 10411–10421, 2001. 22249

Bekki, S., Bodeker, G., Bais, A. F., Butchart, N., Eyring, V., Fahey, D., Kinnison, D. E., Langematz, U., Mayer, B., Portmann, R., Rozanov, A., Braesicke, P., Charlton-Perez, A. J., Chubarova, N. E., Cionni, I., Diaz, S. B., Gillett, R., Giorgetta, M. A., Komala, N., Lefevre, F.,

ACPD
14, 22245–22272, 2014

McLandress, C., Perlwitz, J., Peter, T., and Shibata, K.: Future ozone and its impact on surface UV, in: Scientific Assessment of Ozone Depletion: 2010, Global Ozone Research and Monitoring Project – Report No. 52, 516 pp., World Meteorological Organization, Geneva, Switzerland, 2011. 22248

Bevilacqua, R. M., Aellig, C. P., Debrestian, D., Fromm, M., Hoppel, K., Lumpe, J., Shettle, E., Hornstein, J., Randall, C., Rusch, D., and Rosenfield, J. E.: POAM II ozone observations in the Antarctic ozone hole in 1994, 1995, and 1996, J. Geophys. Res., 102, 23643–23657, 1997. 22249, 22264

Chen, H.-Y., Lien, C.-Y., Lin, W.-Y., Lee, Y. T., and Lin, J. J.: UV absorption cross sections of ClOOCl are consistent with ozone degradation models, Science, 324, 781–784, 2009. 22249

Frieler, K., Rex, M., Salawitch, R. J., Canty, T., Streibel, M., Stimpfle, R. M., Pfeilsticker, K., Dorf, M., Weisenstein, D. K., and Godin-Beekmann, S.: Toward a better quantitative understanding of polar stratospheric ozone loss, Geophys. Res. Lett, 33, L10812, doi:10.1029/2005GL025466, 2006. 22250, 22264

Hassler, B., Daniel, J. S., Johnson, B. J., Solomon, S., and Oltmans, S.: An assessment of changing ozone loss rates at South Pole: Twenty-five years of ozonesonde measurements, J. Geophys. Res., 116, D22301, doi:10.1029/2011JD016353, 2011. 22249, 22264

Hoppel, K., Bevilacqua, R., Canty, T., Salawitch, R., and Santee, M.: A measurement/model comparison of ozone photochemical loss in the Antarctic ozone hole using Polar ozone and aerosol measurement observations and the match technique, J. Geophys. Res., 110, D19304, doi:10.1029/2004JD005651, 2005. 22249, 22264

Kalnajs, L. E. and Avallone, L. M.: A novel lightweight low-power dual-beam ozone photometer utilizing solid-state optoelectronics, J. Atmos. Ocean. Tech., 27, 869–880, 2010. 22250

Klekociuk, A. R., Tully, M. B., Alexander, S. P., Dargaville, R. J., Deschamps, L. L., Fraser, P. J., Gies, H. P., Henderson, S. I., Javorniczky, J., Krummel, P. B., Petelina, S. V., Shanklin, J. D., Siddaway, J. M., and Stone, K. A.: The Antarctic ozone hole during 2010, Aust. Met. Oceanogr. J., 61, 253–267, 2011. 22253

Kohma, M. and Sato, K.: Simultaneous occurrence of polar stratospheric clouds and upper-tropospheric clouds caused by blocking anticyclones in the Southern Hemisphere, Atmos. Chem. Phys., 13, 3849–3864, doi:10.5194/acp-13-3849-2013, 2013. 22248, 22255

Kremser, S., Schofield, R., Bodeker, G. E., Connor, B. J., Rex, M., Barret, J., Mooney, T., Salawitch, R. J., Canty, T., Frieler, K., Chipperfield, M. P., Langematz, U., and Feng, W.: Retrievals

ACPD
14, 22245–22272, 2014

of chlorine chemistry kinetic parameters from Antarctic ClO microwave radiometer measurements, Atmos. Chem. Phys., 11, 5183–5193, doi:10.5194/acp-11-5183-2011, 2011. 22249
Kuttippurath, J., Goutail, F., Pommereau, J. P., Lefevre, F., Roscoe, H. K., Pazmino, A., Feng, W., Chipperfield, M. P., and Godin-Beekmann, S., Estimation of Antarctic ozone loss from ground-based total column measurements, Atmos. Chem. Phys., 10, 6569–6581, doi:10.5194/acp-10-6569-2010, 2010. 22250
Molina, L. and Molina, M.: Production of Cl_2O_2 from the self-reaction of the ClO radical, J. Phys. Chem., 91, 433–436, 1987. 22248
Papanastasiou, D. K., Papadimitriou, V. C., Fahey, D. W., and Burkholder, J. B.: UV Absorption Spectrum of the ClO Dimer (Cl_2O_2) between 200 and 420 nm, J. Phys. Chem.-USA, 113, 13711–13726, 2009. 22249
Pitts, M. C., Poole, L. R., and Thomason, L. W.: CALIPSO polar stratospheric cloud observations: second-generation detection algorithm and composition discrimination, Atmos. Chem. Phys., 9, 7577–7589, doi:10.5194/acp-9-7577-2009, 2009. 22255
Plenge, J., Flesch, R., Kühl, S., Vogel, B., Müller, R., Stroh, F., and Rühl, E.: Ultraviolet photolysis of the ClO dimer, J. Phys. Chem.-USA, 108, 4859–4863, 2004. 22249
Pope, F. D., Hansen, J. C., Bayes, K. D., Friedl, R. R., and Sander, S. P.: Ultraviolet absorption spectrum of chlorine peroxide, ClOOCl, J. Phys. Chem.-USA, 111, 4322–4332, 2007. 22249
Rabier, F., Cohn, S., Cocquerez, P., Hertzog, A., Avallone, L., Deshler, T., Haase, J., Hock, T., Doerenbecher, A., Wang, J., Guidard, V., Thépaut, J.-N., Langland, R., Tangborn, A., Balsamo, G., Brun, E., Parsons, D., Bordereau, J., Cardinali, C., Danis, F., Escarnot, J.-P., Fourrié, N., Gelaro, R., Genthon, C., Ide, K., Kalnajs, L., Martin, C., Meunier, L.-F., Nicot, J.-M., Perttula, T., Potts, N., Ragazzo, P., Richardson, D., Sosa-Sesma, S., and Vargas, A.: The Concordiasi field experiment over Antarctica: first results from innovative atmospheric measurements, B. Am. Meterol. Soc., 94, ES17–ES20, 2013. 22250
Rex, M., von der Gathen, P., Harris, N., Lucic, D., Knudsen, B., Braathen, G., Reid, S., de Backer, H., Claude, H., and Fabian, R.: In situ measurements of stratospheric ozone depletion rates in the Arctic winter 1991/1992: a Lagrangian approach, J. Geophys. Res., 103, 5843–5853, 1998. 22249
Rex, M., von der Gathen, P., Braathen, G., Harris, N., Reimer, E., Beck, A., Alfier, R., Kruger-Carstensen, R., Chipperfield, M., de Backer, H., Balis, D., O'Connor, F., Dier, H., Dorokhov, V., Fast, H., Gamma, A., GIL, M., Kyro, E., Litynska, Z., Mikkelsen, S., Molyneux, M., Murphy,

ACPD
14, 22245–22272, 2014

G., Reid, S., Rum- mukainen, M., and Zerefos, C.: Chemical ozone loss in the Arctic winter 1994/95 as determined by the Match technique, J. Atmos. Chem., 32, 35–59, 1999. 22252

Rex, M., Salawitch, R., Harris, N., von der Gathen, P., Braathen, G., Schulz, A., Deckelmann, H., Chipperfield, M., Sinnhuber, B., Reimer, E., Alfier, R., Bevilacqua, R., Hoppel, K., Fromm, M., Lumpe, J., Kullmann, H., Kleinbohl, A., Bremer, H., von Konig, M., Kunzi, K., Toohey, D., Vömel, H., Richard, E., Aikin, K., Jost, H., Greenblatt, J., Loewenstein, M., Podolske, J., Webster, C., Flesch, G., Scott, D., Herman, R., Elkins, J., Ray, E., Moore, F., Hurst, D., Romashkin, P., Toon, G., Sen, B., Margitan, J., Wennberg, P., Neuber, R., Allart, M., Bojkov, B., Claude, H., Davies, J., Davies, W., de Backer, H., Dier, H., Dorokhov, V., Fast, H., Kondo, Y., Kyro, E., Litynska, Z., Mikkelsen, I., Molyneux, M., Moran, E., Nagai, T., Nakane, H., Parrondo, C., Ravegnani, F., Skrivankova, P., Viatte, P., and Yushkov, V.: Chemical depletion of Arctic ozone in winter 1999/2000, J. Geophys. Res., 107, 8276, doi:10.1029/2001JD000533, 2002. 22249

Sander, S. P., Friedl, R., Golden, D., Kurylo, M. J., Wine, P. H., Abbatt, J., Burkholder, J. B., Kolb, C. E., Moortgat, G. K., Huie, R. E., and Orkin, V. L.: Chemical kinetics and photochemical data for use in atmospheric studies, JPL Publication 10-6, Jet Propulsion Laboratory, Pasadena, 2011. 22249

Santee, M. L., Lambert, A., Read, W. G., Livesey, N. J., Manney, G. L., Cofield, R. E., Cuddy, D. T., Daffer, W. H., Drouin, B. J., Froidevaux, L., Fuller, R. A., Jarnot, R. F., Knosp, B. W., Perun, V. S., Snyder, W. V., Stek, P. C., Thurstans, R. P., Wagner, P. A., Waters, J., Connor, B., Urban, J., Murtagh, D., Ricaud, P., Barret, B., Kleinboehl, A., Kuttippurath, J., Kuellmann, H., von Hobe, M., Toon, G. C., and Stachnik, R. A.: Validation of the Aura microwave limb sounder ClO measurements, J. Geophys. Res.-Atmos., 113, D15S22, doi:10.1029/2007JD008762, 2008. 22255

Santee, M. L., Sander, S. P., Livesey, N. J., and Froidevaux, L.: Atmospheric Chemistry Special Feature: Constraining the chlorine monoxide (ClO)/chlorine peroxide (ClOOCl) equilibrium constant from Aura Microwave Limb Sounder measurements of nighttime ClO, P. Natl. Acad. Sci. USA, 107, 6588–6593, 2010. 22249

Schofield, R., Frieler, K., Wohltmann, I., Rex, M., von Hobe, M., Stroh, F., Koch, G., Peter, T., Canty, T., Salawitch, R., and Volk, C. M.: Polar stratospheric chlorine kinetics from a self-match flight during SOLVE-II/EUPLEX, Geophys. Res. Lett, 35, L01807, doi:10.1029/2007GL031740, 2008. 22249

ACPD
14, 22245–22272, 2014

Shindell, D. and deZafra, R.: Chlorine monoxide in the Antarctic spring vortex, 2. A comparison of measured and modeled diurnal cycling over McMurdo Station, 1993, J. Geophys. Res., 101, 1475–1487, 1996. 22249
Solomon, P., Connor, B., Barrett, J., Mooney, T., Lee, A., and Parrish, A.: Measurements of stratospheric ClO over Antarctica in 1996–2000 and implications for ClO dimer chemistry, Geophys. Res. Lett., 29, 1708, doi:10.1029/2002GL015232, 2002. 22249
Solomon, S.: Stratospheric ozone depletion: a review of concepts and history, Rev. Geophys., 37, 275–316, 1999. 22248
Sonkaew, T., von Savigny, C., Eichmann, K.-U., Weber, M., Rozanov, A., Bovensmann, H., Burrows, J. P., and Grooß, J.-U.: Chemical ozone losses in Arctic and Antarctic polar winter/spring season derived from SCIAMACHY limb measurements 2002–2009, Atmos. Chem. Phys., 13, 1809–1835, doi:10.5194/acp-13-1809-2013, 2013. 22249, 22264
Stimpfle, R. M., Wilmouth, D. M., Salawitch, R. J., and Anderson, J. G.: First measurements of ClOOCl in the stratosphere: the coupling of ClOOCl and ClO in the Arctic polar vortex, J. Geophys. Res., 109, D03301, doi:10.1029/2003JD003811, 2004. 22249
Thompson, D. W. J. and Solomon, S.: Interpretation of recent Southern Hemisphere climate change, Science, 296, 895–899, doi:10.1126/science.1069270, 2002. 22248
Thompson, D. W. J., Solomon, S., Kushner, P. J., England, M. H., Grise, K. M., and Karoly, D. J.: Signatures of the Antarctic ozone hole in Southern Hemisphere surface climate change, Nat. Geosci., 4, 741–749, 2011. 22247
Vogel, B., Grooß, J. U., Müller, R., Deshler, T., Karhu, J., McKenna, D. S., Müller, M., Toohey, D., Toon, G. C., and Stroh, F.: Vertical profiles of activated ClO and ozone loss in the Arctic vortex in January and March 2000: In situ observations and model simulations, J. Geophys. Res.-Atmos., 108, 8334, doi:10.1029/2002JD002564, 2003. 22249
von Hobe, M., Grooß, J.-U., Müller, R., Hrechanyy, S., Winkler, U., and Stroh, F.: A re-evaluation of the ClO/Cl_2O_2 equilibrium constant based on stratospheric in-situ observations, Atmos. Chem. Phys., 5, 693–702, doi:10.5194/acp-5-693-2005, 2005. 22249
von Hobe, M., Salawitch, R. J., Canty, T., Keller-Rudek, H., Moortgat, G. K., Grooß, J.-U., Müller, R., and Stroh, F.: Understanding the kinetics of the ClO dimer cycle, Atmos. Chem. Phys., 7, 3055–3069, doi:10.5194/acp-7-3055-2007, 2007. 22249
von Hobe, M., Stroh, F., Beckers, H., Benter, T., and Willner, H.: The UV/Vis absorption spectrum of matrix-isolated dichlorine peroxide, ClOOCl, Phys. Chem. Chem. Phys., 11, 1571–1580, 2009. 22249

ACPD
14, 22245–22272, 2014

Wang, Z., Stephens, G., Deshler, T., Trepte, C., Parish, T., Vane, D., Winker, D., Liu, D., and Adhikari, L.: Association of Antarctic polar stratospheric cloud formation on tropospheric cloud systems, Geophys. Res. Lett., 35, L13806, doi:10.1029/2008GL034209, 2008. 22254

Ward, S. M., Deshler, T., and Hertzog, A.: Quasi-Lagrangian measurements of nitric acid trihydrate formation over Antarctica, J. Geophys. Res.-Atmos., 119, 245–258, 2014. 22251

Wilmouth, D. M., Hanisco, T. F., Stimpfle, R. M., and Anderson, J. G.: Chlorine-catalyzed ozone destruction: Cl atom production from ClOOCl photolysis, J. Phys. Chem.-USA, 113, 14099–14108, 2009. 22249

Wohltmann, I. and Rex, M.: Improvement of vertical and residual velocities in pressure or hybrid sigma-pressure coordinates in analysis data in the stratosphere, Atmos. Chem. Phys., 8, 265–272, doi:10.5194/acp-8-265-2008, 2008. 22252

ACPD
14, 22245–22272, 2014

Table 1. Details of balloon flights analysed for ozone loss rates.

	PSC-14	PSC-16	PSC-17
Instrument	LMDOz	UCOz	UCOz
Launch date	5 Sep 03:10 UT	11 Sep 03:00 UT	14 Sep 01:50 UT
Last data record	21 Dec 14:28 UT	4 Oct	15 Oct
Distance travelled (km)	147 500	34 565	59 034
Days used to calculate	259–269	255–275	259–277
ozone loss rates	16–23 Sep	12 Sep–2 Oct	16 Sep–4 Oct
Theta range (K)	404–425	416–437	414–436
Pressure range (hPa)	62–66	62–69	64–69

ACPD
14, 22245–22272, 2014

Table 2. Comparison of Antarctic stratospheric ozone loss rates.

Method	Time	Area	Ozone loss rate (ppbv day^{-1}) (ppbv (sunlit h)$^{-1}$)*	Reference
Concordiasi (410–430 K)	12–22 Sep: 2010	vortex-average	74 ± 70 6 ± 6*	This work
POAM II (500 K)	1–30 Sep: 1994, 1995, 1996	vortex-average	85 ± 15	Bevilacqua et al. (1997, Fig. 9)
POAM III (445–523 K)	1–15 Sep: 1998–2003	vortex-average	8 ± 6*	Hoppel et al. (2005, Fig. 9)
Ozonesondes (500 K)	15 Aug–15 Sep: 2003	vortex-average	4 ± 1*	Frieler et al. (2006, Fig. 1)
Ozonesondes (475–500 K)	23 Aug–27 Sep: 1991–1995 1996–2010	89.98° S	90 ± 10 70 ± 10	Hassler et al. (2011, Fig. 5)
SCIAMACHY (475 K)	18 Aug–18 Sep: 2002–2008	vortex-average	45 ± 6	Sonkaew et al. (2013)
Average	1991–1995 1996–2010		88 ± 18 54 ± 16	

Uncertainties given as 1 standard deviation.

ACPD
14, 22245–22272, 2014

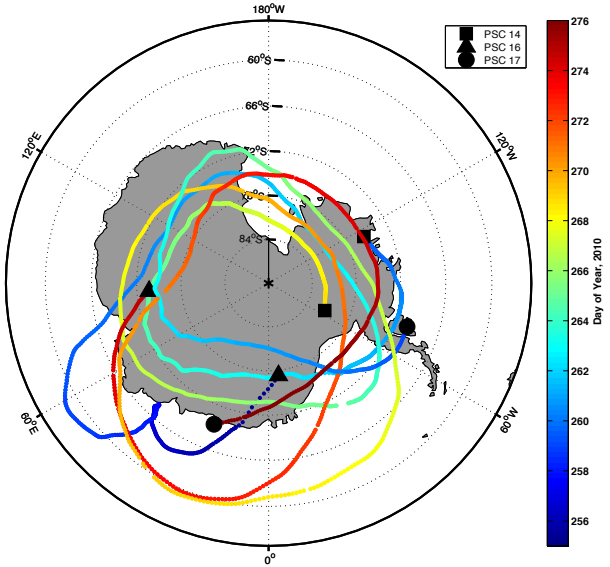

Figure 1. The flight paths of the three ozone Concordiasi balloons are displayed.

ACPD
14, 22245–22272, 2014

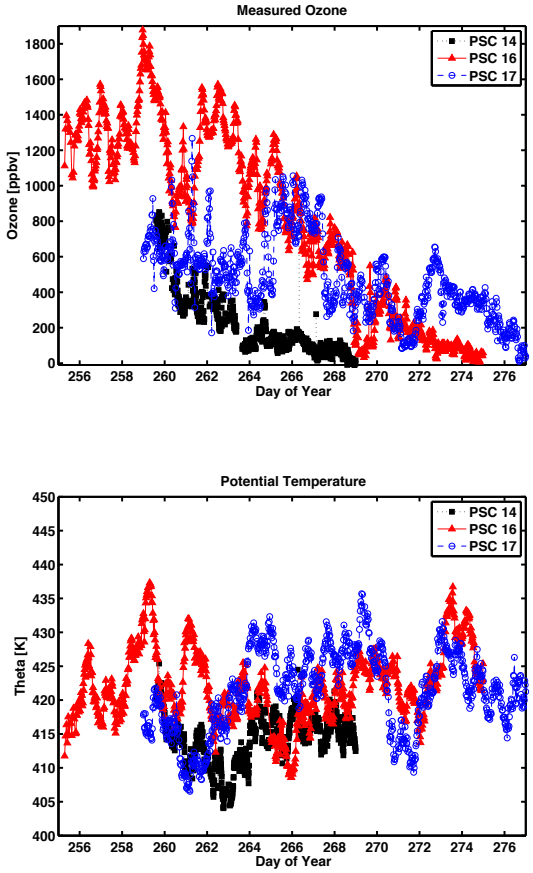

Figure 2. Ozone and potential temperature along the trajectory of each of the ozone instrumented Concordiasi balloons. Clearly measured is the ozone loss under perturbed springtime conditions. The diurnal heating and cooling of the balloon is evident in the potential temperature variations.

ACPD
14, 22245–22272, 2014

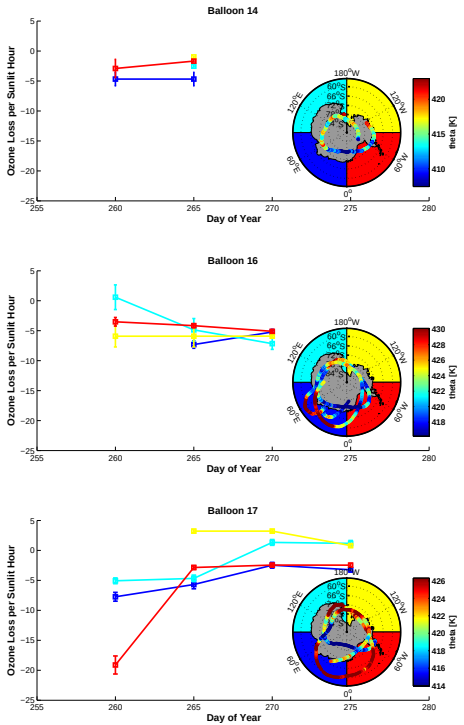

Figure 3. Ozone loss per sunlit hour for all of the matches for each of the ozone instrumented Concordiasi balloon flights. The matches are binned into the longitude quadrant of their end match (blue: 0–90° E, turquoise: 90–180° E, yellow 90–180° W and red 0–90° W). While each match requires the potential temperature to be within 1 K, all matches with an initial or end match within ±5 days are binned to give the ozone vs. sunlit hour regression shown. This way a match ending on day 263 will be represented in both the 260 and 265 data points above. The colour bar is used to indicate the potential temperature of the ozone observations as plotted with dots on the map.

ACPD
14, 22245–22272, 2014

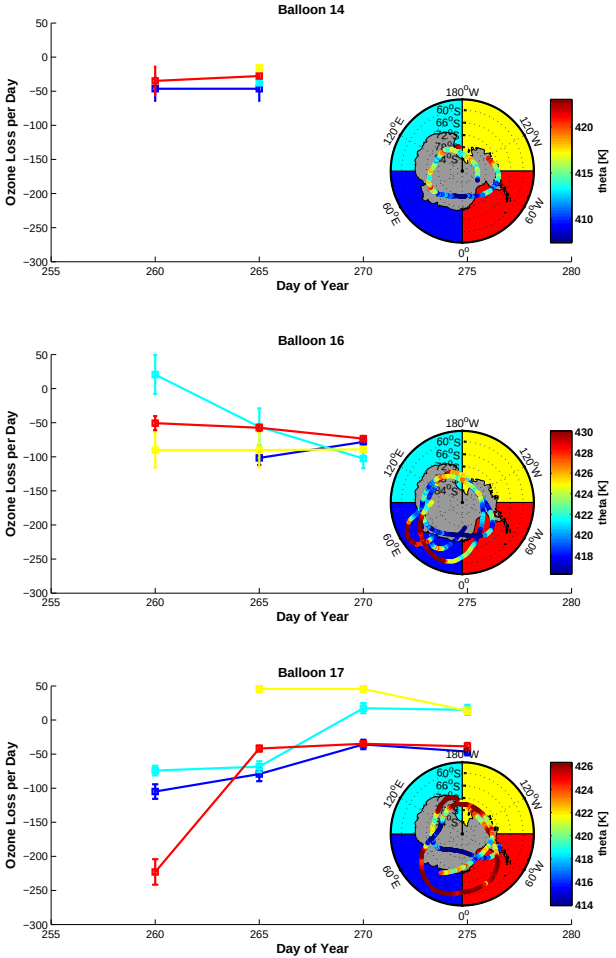

Figure 4. As Fig. 3 but for ozone loss per day.

ACPD
14, 22245–22272, 2014

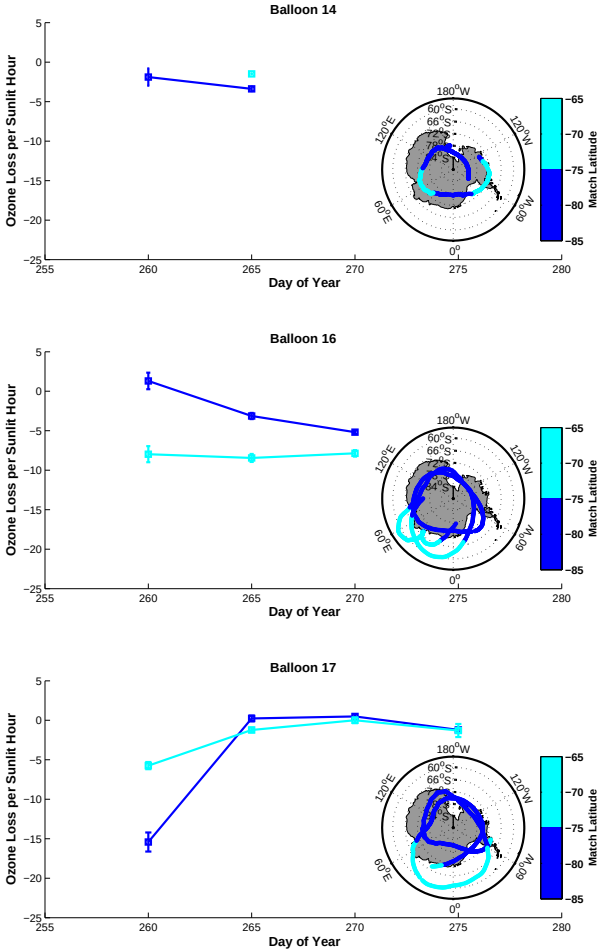

Figure 5. Ozone losses binned according to mean latitude of the match.

ACPD
14, 22245–22272, 2014

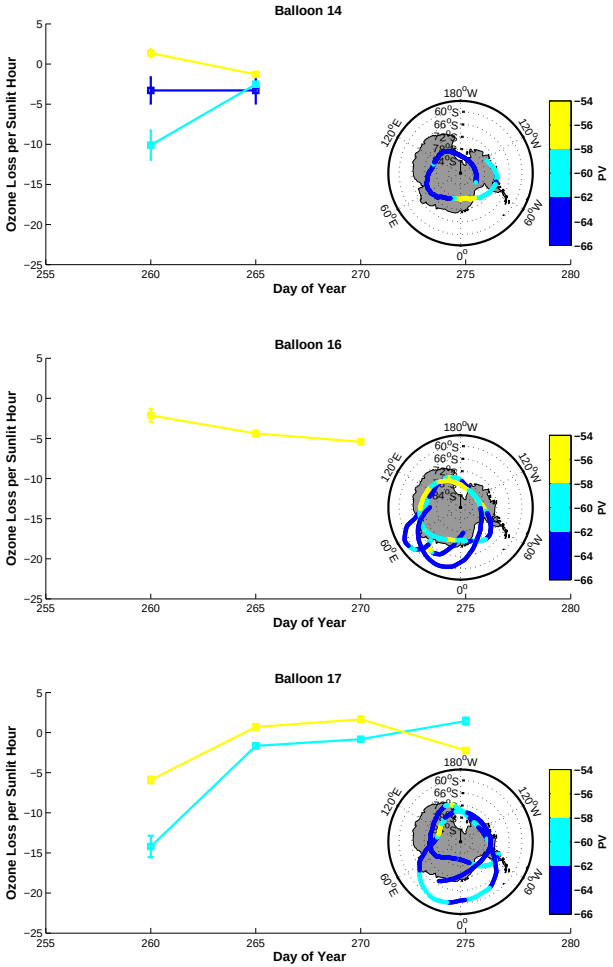

Figure 6. Ozone loss according to mean normalised PV of the match.

ACPD
14, 22245–22272, 2014

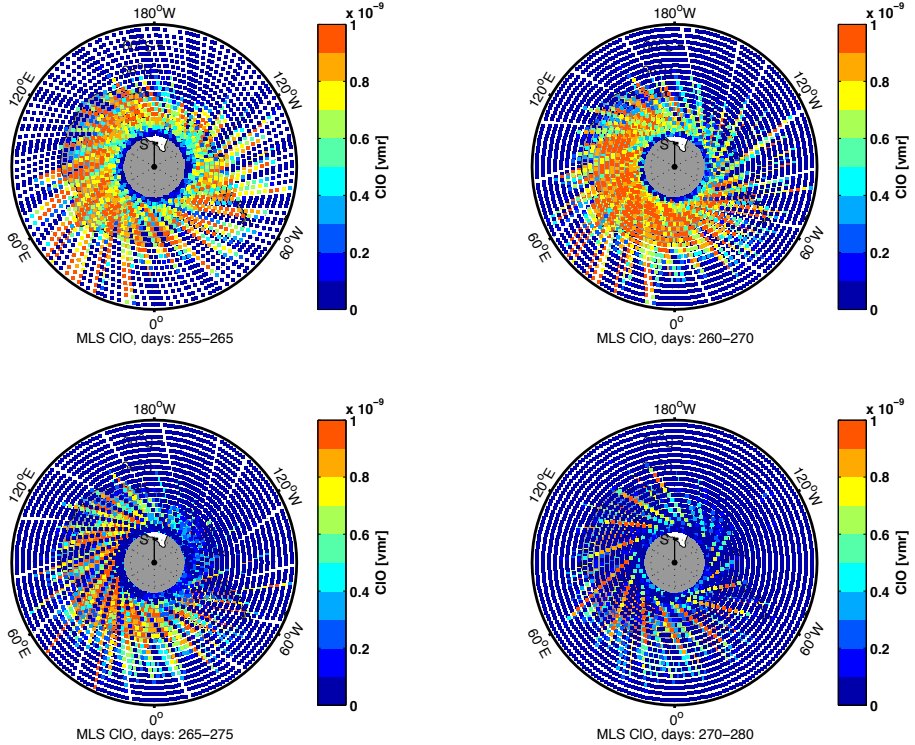

Figure 7. Microwave Limb Sounder ClO data retrieved on the 68.13 hPa level over the ten day periods used for the four ozone loss calculations in Figs. 3 and 4.

ACPD
14, 22245–22272, 2014

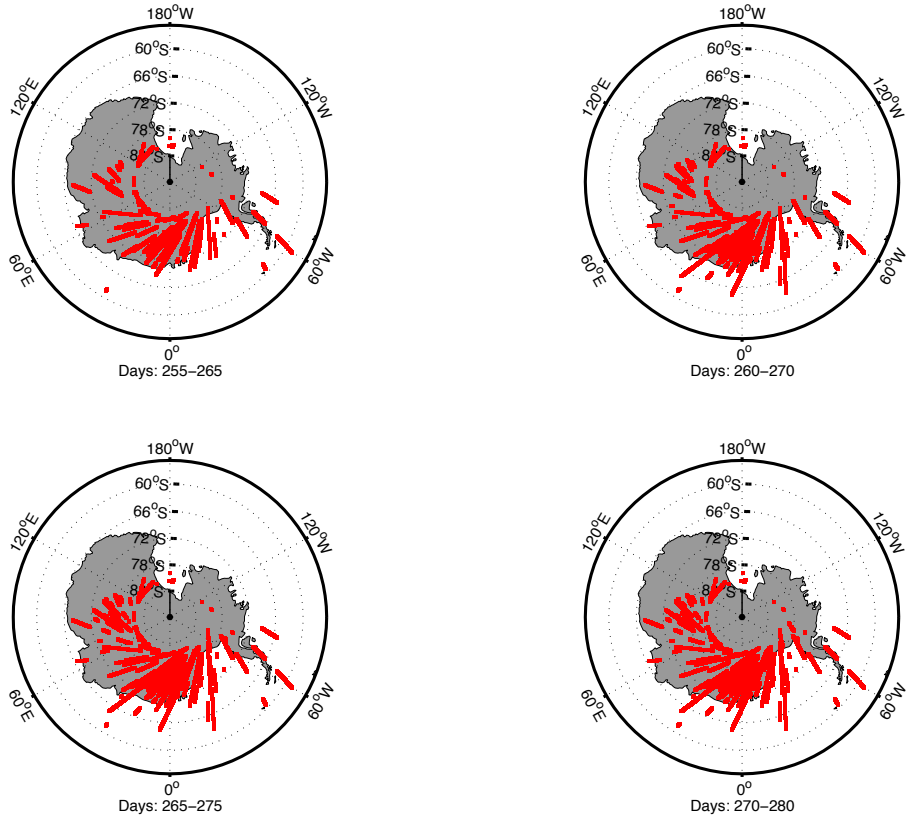

Figure 8. Calipso PSC flag over the 10 day bin intervals used in the ozone loss calculations for the 16.7 km altitude layer.

ACPD
14, 22245–22272, 2014